Journal of Applied Physics ARTICLE scitation.org/journal/jap

Role of minority charge carriers in the formation of the thermo-electromotive force in *p*-type silicon

Cite as: J. Appl. Phys. **133**, 195106 (2023); doi: 10.1063/5.0149876
Submitted: 9 March 2023 · Accepted: 5 May 2023 ·
Published Online: 19 May 2023

André Siewe Kamegni[a] and Igor Lashkevych[b]

AFFILIATIONS

Instituto Politécnico Nacional, UPIITA, Av. IPN, No. 2580, col. La Laguna Ticoman, del. Gustavo A. Madero, C.P. 07340 Mexico, CDMX, Mexico

Note: This paper is part of the Special Topic on Semiconductor Physics: Plasma, Thermal, Elastic, and Acoustic Phenomena.
[a]**Author to whom correspondence should be addressed:** siewekamegni@yahoo.fr
[b]ilashkevych@ipn.mx and i32555@gmail.com

ABSTRACT

The contribution of minority charge carriers (electrons) is taken into account in the evaluation of thermo-electromotive force (thermo-E.M.F.) of a non-degenerate *p*-type semiconductor in the stationary state and when the quasi-neutrality condition is fulfilled. The results obtained show that the contribution to the thermo-E.M.F. due to the presence of minority electrons is a function of the bandgap and the length of the semiconductor used. It also depends on the minority carriers through their electrical conductivity, thermal conductivity, Seebeck coefficient, and bulk and surface recombinations. That contribution tends to reduce the principal thermo-E.M.F. ($\alpha_p \Delta T$) of the *p*-type semiconductor and will, therefore, be called counter-thermo-electromotive force (counter-thermo-E.M.F.). The calculations made in the case of silicon give a counter-thermo-E.M.F. of magnitude generally non-negligible, which decreases when the length of the silicon and the concentration of doping elements increase. Finally, it is shown that the best way to minimize the counter-thermo-E.M.F. is to treat the surface of the semiconductor to promote the recombination of minority carriers there.

I. INTRODUCTION

The current environmental and technological concerns are pushing researchers to invest in the development of renewable energy sources and to create electronic devices energetically autonomously capable of operating in extreme and remote areas such as polar zones, other solar system planets, and deep space. Also, the need to recycle waste energy in the form of heat (which represents more than 60% of the energy produced in American industries[1,2] and about 30% in France[3]) is becoming more and more important as it could considerably reduce the world energy demand.

Thermoelectric generators (TEGs), the ideal candidate to solve precedent issues, have drawn significant attention during the recent decades for their multiple advantages: they produce green energy, do not require any maintenance service after installation, have no moving parts, and can, therefore, be installed near mechanically sensitive devices. But for TEGs to be a little more competitive with other forms of energy production, three main challenges must be addressed: the synthesis of thermoelectric materials must be as non-toxic as possible;[4,5] the elements that make up the thermoelectric materials must be available to consider large-scale production;[6,7] and the thermoelectric efficiency of known materials must be improved or new materials with better efficiency must be discovered.[4,8] According to Refs. 9 and 10, this last challenge could be achieved if the dimensionless figure of merit of the materials is around $zT = 4$. The present study is part of those works carried out or in progress whose aim is trying to meet the third challenge of the previous list. Its main contribution is the development of a fine theory able to give in more detail the thermoelectric description in *p*-type materials and determine the potential effects that can prevent the optimization of their thermoelectric efficiency and mostly how these effects could be stopped or reduced.

To manufacture a TEG, one needs at least an *n*-type and a *p*-type semiconductor of comparable performance.[8] A study focused on the role of minority charge carriers in the formation of the thermo-E.M.F. in an *n*-type material has recently been carried out.[11] The authors show that the presence of that type of carrier can contribute positively, negatively, or have no action on the total thermo-E.M.F. depending on the width of the bandgap, the

concentration of carriers, recombination mechanisms, etc. But, in the case of silicon, the magnitude of that contribution is generally very weak and can be neglected. What about the role of minority carriers on the formation of thermo-E.M.F. in a p-type semiconductor? In many books dedicated to the physics of semiconductors and the theoretical description of thermoelectric effects, it is common to study the n-type semiconductor and say that the results corresponding to p-type semiconductor can be obtained by conjecture (by changing the sign of the electric charge and the index of the physical quantities n to p or e to h).[12–15] Reference 16 nevertheless draws attention to the possible errors made when making such deductions. The authors show, for example, that such a conjecture cannot be applied to the description of charge transport in a semiconductor sandwiched between two thin metal layers because of the role played by surface recombination processes that are of paramount importance when the semiconductor is p-type.

In this work, the contribution due to electrons (minority charge carriers) to the thermo-E.M.F. of a non-degenerate p-type semiconductor of length $2d$, sandwiched between two thin metal layers, will be expressed. The computation will be done focusing on the case of silicon. It is one of the most promising thermoelectric materials because of its high power factor[17] and abundance in the Earth's crust.[18,19] Its synthesis is also non-toxic.

II. TRANSPORT COEFFICIENTS COMPUTATIONS

In the context of this study, a p-type semiconductor is a semiconductor whose holes constitute the majority charge carriers and the minority carriers are constituted by electrons. It is a semiconductor characterized by $p_0 \gg n_0$, where p_0 (n_0) is the concentration of holes (electrons) at equilibrium and temperature $T_0 = \frac{T_h+T_c}{2}$. Here, T_h is the temperature of the heat source soldered to one end of the semiconductor. At the other end is attached a heat sink at temperature T_c. The cross sections are assumed to be uniform with unit area and the lateral faces adiabatically isolated. Although the equations established in this article can be applied to other non-degenerate semiconductor thermoelectric materials with the characteristics quoted above, the computations of contribution to thermo-E.M.F. due to minority electrons will be made only for p-type silicon. For that specific material, the transport coefficients are calculated assuming that there are no donor elements in the sample ($N_D = 0$); the concentration of holes at temperature T_0 is equal to the concentration of acceptors ($p_0 = N_A$) and the concentration of electrons given by the relation $n_0 = n_i^2/p_0$. The quantity n_i designates the intrinsic concentration, which is defined as[20,21]

$$n_i = (N_v \times N_c)^{\frac{1}{2}} \exp\left(-\frac{\varepsilon_{g0}}{2k_B T_0}\right) \quad (\mathrm{cm}^{-3}), \tag{1}$$

where N_c (N_v) represents the effective density of states in the conduction band (in the valence band), k_B is the Boltzmann coefficient, and ε_{g0} is the width of the bandgap of the silicon and can be calculated following Thurmond's model,[22,23]

$$\varepsilon_{g0} = 1.17 - 4.73 \times 10^{-4} \times \frac{T_0^2}{T_0 + 636} \quad (\mathrm{eV}). \tag{2}$$

From Boltzmann's transport equation and for non-degenerate p-silicon ($N_A < 10^{19}\ \mathrm{cm}^{-3}$), the Seebeck coefficients of electrons α_n and holes α_p can be expressed as[24,25]

$$\alpha_n = -\frac{k_B}{e}\left[r_n + \frac{5}{2} + \ln\left(\frac{N_c}{n_0}\right)\right], \tag{3}$$

$$\alpha_p = \frac{k_B}{e}\left[r_p + \frac{5}{2} + \ln\left(\frac{N_v}{p_0}\right)\right], \tag{4}$$

where the parameters r_n and r_p are energy exponents in the relaxation time-energy relation in the conduction band and the valence band, respectively. Their value depends on the predominant scattering mechanism in the considered band. For this study, two values of $r_{n,p}$ will be considered. The first one $r_{n,p} = \frac{3}{2}$ when the carriers are mostly scattered by ionized impurities, and the second value $r_{n,p} = -\frac{1}{2}$ when the scattering mechanism of charge carrier by phonon predominates.[12,26] For silicon and for doping greater than or equal to $N_A = 10^{16}\ \mathrm{cm}^{-3}$, the two preceding scattering mechanisms are predominant; the first for low energy levels and the second for high energy levels.[27–29] The electrical conductivity of electrons σ_n and holes σ_p is calculated from their mobilities b_n and b_p, respectively, and according to the formula,[30,31]

$$\sigma_n = e n_0 b_n; \qquad \sigma_p = e p_0 b_p. \tag{5}$$

The mobilities b_n and b_p are evaluated from the empirical model of Reggiani *et al.*,[32]

$$b = b_0 + \frac{b_L + b_0}{1 + \left(\frac{N_A}{C_r}\right)^a} - \frac{b_1}{1 + \left(\frac{N_A}{C_s}\right)^{-2}} \quad (\mathrm{cm}^2/\mathrm{Vs}), \tag{6}$$

where the acceptor concentration N_A is given in cm^{-3}; $b_L = b_{L0} T_n^{-g+CT_n}$ represents the lattice contribution to the mobility, and it is due to acoustic-and optical-phonon scattering; $T_n = \frac{T_0}{300}$; the other parameters of the model b_{L0}, C, g, b_0, b_1, C_r, C_s, and a are constants or are temperature dependant. Their values that effectively fit the experimental data of carrier mobilities in p-type silicon are shown in Table I. The thermal conductivity κ in silicon is calculated as the sum of three contributions, two of which, κ_n and κ_p, are due to the displacement of charge carriers. According

TABLE I. The parameters of Eq. (6).

Parameters	Electrons	Holes
b_{L0} (cm^2/Vs)	1441.00	470.50
C	0.07	0.00
g	2.45	2.16
b_0 (cm^2/Vs)	$132 \times T_n^{-1.3}$	$44 \times T_n^{-0.8}$
b_1 (cm^2/Vs)	$73.5 \times T_n^{-1.25}$	$28.2 \times T_n^{-0.2}$
C_r (cm^{-3})	$1.22 \times 10^{17} \times T_n^{2.65}$	$2.45 \times 10^{17} \times T_n^{3.1}$
C_s (cm^{-3})	7×10^{20}	6.1×10^{20}
a	0.72	0.719

TABLE II. Values of the dimensionless parameter $\gamma^{(p)}$ for silicon at $T_0 = 300$ K.

N_A (cm^{-3})		10^{16}	10^{17}	10^{18}
$\gamma^{(p)}$	$r_{n,p} = -\frac{1}{2}$	1.0177×10^{15}	1.6735×10^{16}	3.7317×10^{17}
	$r_{n,p} = \frac{3}{2}$	5.0884×10^{14}	8.3676×10^{15}	1.8658×10^{17}

to the Wiedemann–Franz law,[33–35] each of these two contributions is proportional to the temperature and the electrical conductivity of the type of carrier responsible for its creation,

$$\kappa_{n,p} = L\sigma_{n,p}T_0. \tag{7}$$

The proportionality coefficient L called the Lorentz number is defined by $L = \frac{\pi^2}{3}\left(\frac{k_B}{e}\right)^2$. The third contribution κ_{ph} to thermal conduction is due to crystal lattice vibration. For non-degenerate silicon ($N_A < 10^{19}$ cm^{-3}),[17,29,36] κ_{ph} does not depend on electron–phonon interactions but only depends on temperature according to the following empirical relation:[37]

$$\kappa_{ph} = 1585 \times T_0^{-1.23} \qquad (\mathrm{Wcm^{-1}\,K^{-1}}). \tag{8}$$

III. RESULTS AND DISCUSSION

From the model developed in Ref. 38, the expression of the thermo-E.M.F. of a p-type semiconductor in the stationary state and when the condition of quasi-neutrality is fulfilled ($r_d^2 \ll d^2, (L_0^{(p)})^2, (L_S^{(p)})^2$) is given by (See Appendix A for more details)

$$\mathrm{E} = \alpha_p \Delta T + \left(\frac{\sigma_n}{\sigma_p}\alpha_n - \Gamma^{(p)}\right)\Delta T, \tag{9}$$

where r_d represents the Debye length[39,40] defined by $r_d = \sqrt{\frac{\epsilon_s k_B T_0}{e^2(n_0+p_0)}}$, where ϵ_s is the permittivity of the semiconductor. In the case of silicon, the values of r_d are 4.1×10^{-5}, 1.3×10^{-5}, and 4.1×10^{-6} mm corresponding, respectively, to concentrations of dopants equal to 10^{16}, 10^{17}, and 10^{18} cm^{-3}. From (9),

$$\Gamma^{(p)} = \frac{\varepsilon_{g0}}{eT_0}\frac{\frac{L_0^{(p)}}{d}(\gamma^{(p)}+1)\sinh\frac{d}{L_0^{(p)}}}{\frac{L_0^{(p)}}{d}\sinh\frac{d}{L_0^{(p)}} + \gamma^{(p)}\left[\cosh\frac{d}{L_0^{(p)}} + \frac{L_0^{(p)}}{L_S^{(p)}}\sinh\frac{d}{L_0^{(p)}}\right]}. \tag{10}$$

The description model of the thermo-E.M.F. used here has been established considering that the Boltzmann constant is equal to a unit, i.e., $T \equiv k_B T$ and relying on an expression of the energy flux density defined by[41,42]

$$\mathbf{w} = -\kappa\nabla T + \sum_{i=\{n,p\}}(\tilde{\varphi}_i + \pi_i)\mathbf{j}_i, \tag{11}$$

where $\tilde{\varphi}_i$, π_i, and $\mathbf{j}_i$ are, respectively, the electrochemical potential, the Peltier, and electrical current density of i-type carriers. Equation (11) is valid only if $\kappa \equiv \frac{\kappa}{k_B}$ and $\pi_i \equiv \frac{\pi_i}{k_B}$. Taking into account the above and considering that $n_0 \ll p_0$, the dimensionless parameter $\gamma^{(p)}$ is written in the following form (refer to Appendix B):

$$\gamma^{(p)} = \frac{e^2}{\xi\varepsilon_{g0}\sigma_n}\frac{\kappa}{k_B}, \tag{12}$$

where $\xi = r_n + r_p + 5$ and κ is the total thermal conductivity that is defined as the sum of its three contributions,

$$\kappa = \kappa_n + \kappa_p + \kappa_{ph}. \tag{13}$$

The results of the calculation of the parameter $\gamma^{(p)}$ for three values of the dopant concentration are shown in Table II below. For all the three values of concentration of acceptor elements considered, $\gamma^{(p)} \gg 1$ either for the energy levels where the phonon scattering mechanism predominates ($r_{n,p} = -\frac{1}{2}$) or for those where the carriers are mostly scattered by ionized impurities ($r_{n,p} = -\frac{3}{2}$). The p-type silicon is, thus, a semiconductor with very high thermal conductivity according to the classification given in Ref. 38. The diffusion length $L_0^{(p)}$ and characteristic length $L_S^{(p)}$ of that type of semiconductors can be written as follows:[33,38] $L_0^{(p)} = \frac{1}{e}\sqrt{\tau_0 T_0 \frac{n_0+p_0}{n_0 p_0}\frac{\sigma_n\sigma_p}{(\sigma_n+\sigma_p)}}$ and $L_S^{(p)} = \frac{T_0}{e^2 S}\frac{n_0+p_0}{n_0 p_0}\frac{\sigma_n\sigma_p}{(\sigma_n+\sigma_p)}$, where S represents the surface recombination velocity and τ_0 refers to the lifetime of charge carriers defined as follows: $\frac{1}{\tau_0} = \frac{1}{\tau_{bb}} + \frac{1}{\tau_{SRH}}$. When there are no trapping centers in the semiconductor structure, only band-to-band recombination exists and the carrier's lifetime is $\tau_0 = \tau_{bb}$.[43] For a semiconductor with an indirect bandgap like silicon and containing N_t cm^{-3} of recombination centers in its crystal structure, solely Shockley–Read–Hall recombination is present and the carrier lifetime is $\tau_0 = \tau_{SRH}$.[44] If, moreover, the semiconductor is p-type, $\tau_0 = \tau_n = \frac{1}{k_n N_t}$ (demonstration in Appendix C), where τ_n is the lifetime of minority electrons[15,45] and k_n is their capture coefficient. For silicon doping between 10^{14} and 10^{18} cm^{-3}, the minority carrier lifetime can be calculated as a function of N_A using Kendall's empirical model:[46] $\tau_n = \frac{\tau_{n0}}{1+\frac{N_A}{N_{A0}}}$, where τ_{n0} and N_{A0} represent two constants whose values bring the model closer to the experimental results. Taking into account the considerations use in Eq. (12), the diffusion length and characteristic length are reduced to

$$L_0^{(p)} = \sqrt{\frac{\tau_n k_B T_0 b_n}{e}}, \tag{14}$$

$$L_S^{(p)} = \frac{k_B T_0 b_n}{eS}. \tag{15}$$

The diffusion length and characteristic length do not dependent on majority carriers. They depend on the minority carriers through their mobility, their lifetime, and their surface recombination rate. The results of the calculation of the diffusion length of silicon type p are given in Table III. The diffusion length values are independent of the predominant scattering mechanism and are all less than 1 mm. As reported in Ref. 38, decreasing the length of the p-type semiconductor sample with respect to the diffusion length is not sufficient to allow the reduction in the minority carriers' contribution to the

TABLE III. Values of minority carrier lifetime and diffusion length for three dopant concentrations in *n*-type silicon at $T_0 = 300$ K.

N_A (cm^{-3})	10^{16}	10^{17}	10^{18}
$\tau_n^{(p)}$ (s)	10^{-4}	5×10^{-5}	6×10^{-6}
$L_0^{(p)}$ (mm)	0.5699	0.3143	0.0729

thermo-E.M.F. like in an *n*-type semiconductor.[11] From Eq. (9), the contribution to the thermo-E.M.F. due to the presence of minority electrons can be written as follows:

$$\mathrm{E}_n = \left(\frac{\sigma_n}{\sigma_p}\alpha_n - \frac{\varepsilon_{g0}}{eT_0}\frac{1}{\frac{1}{\gamma^{(p)}} + \frac{d}{L_S^{(p)}} + \frac{d}{L_0^{(p)}}\coth\frac{d}{L_0^{(p)}}}\right)\Delta T. \tag{16}$$

That contribution is always opposite to the classical thermo-E.M.F. of the *p*-type semiconductor. In no case can it have the same sign as $\alpha_p \Delta T$, and therefore, it will be called in the rest of this article the counter-thermo-E.M.F. If $d \ll L_0^{(p)}, L_S^{(p)}$, Eq. (16) becomes

$$\mathrm{E}_n = (\alpha_n - \alpha_p)\Delta T, \tag{17}$$

and the thermo-E.M.F. of the *p*-type semiconductor is written $\mathrm{E} = \alpha_n \Delta T$. In this case, although electrons are minority carriers, they are the only type of carriers involved in the formation of the thermo-E.M.F. This can be physically explained by the fact that the condition $d \ll L_0^{(p)}, L_S^{(p)}$ implies that bulk and surface recombination processes are very weak or absent in the semiconductor (the dwell time of the minority charge carriers in the sample is shorter than their lifetime and the surface recombination rate is low). Now, according to Ref. 16, it is these recombination phenomena that ensure the conversion of the current of the holes $\mathbf{j}_p$ flowing in the *p*-type semiconductor into the current of electrons $\mathbf{j}_n$ that flows in the connecting wires. However, in the absence of these recombinations $j_p = 0$, the semiconductor behaves as if it were *n*-type and the electric current flows in the opposite direction to that expected. If $d \gg L_0^{(p)}$, from Eq. (16), the counter-thermo-E.M.F. in a *p*-type semiconductor is reduced to

$$\mathrm{E}_n = \left(\frac{\sigma_n}{\sigma_p}\alpha_n - \frac{\varepsilon_{g0}}{eT_0}\frac{L_0^{(p)}L_S^{(p)}}{d\left(L_0^{(p)} + L_S^{(p)}\right)}\right)\Delta T. \tag{18}$$

It can be seen from Eq. (18) that the magnitude of the counter-thermo-E.M.F. decreases with the increasing sample length. If, in addition, the surface recombinations are very weak ($L_S^{(p)} \gg L_0^{(p)}$), the relation (18) becomes

$$\mathrm{E}_n = \left(\frac{\sigma_n}{\sigma_p}\alpha_n - \frac{\varepsilon_{g0}}{eT_0}\frac{L_0^{(p)}}{d}\right)\Delta T. \tag{19}$$

Figure 1 shows the variation in $\frac{\mathrm{E}_n}{\alpha_p \Delta T} \times 100$ with half the sample length for concentrations of dopant elements $N_A = 10^{16}$ cm^{-3}, $N_A = 10^{17}$ cm^{-3}, and $N_A = 10^{18}$ cm^{-3}. These curves are plotted in each case for samples of length ranging from $20 \times L_0^{(p)}$ to 80 mm. From that figure, it can be seen that the counter-thermo-E.M.F. given by Eq. (19) cannot be neglected for the case of weak surface

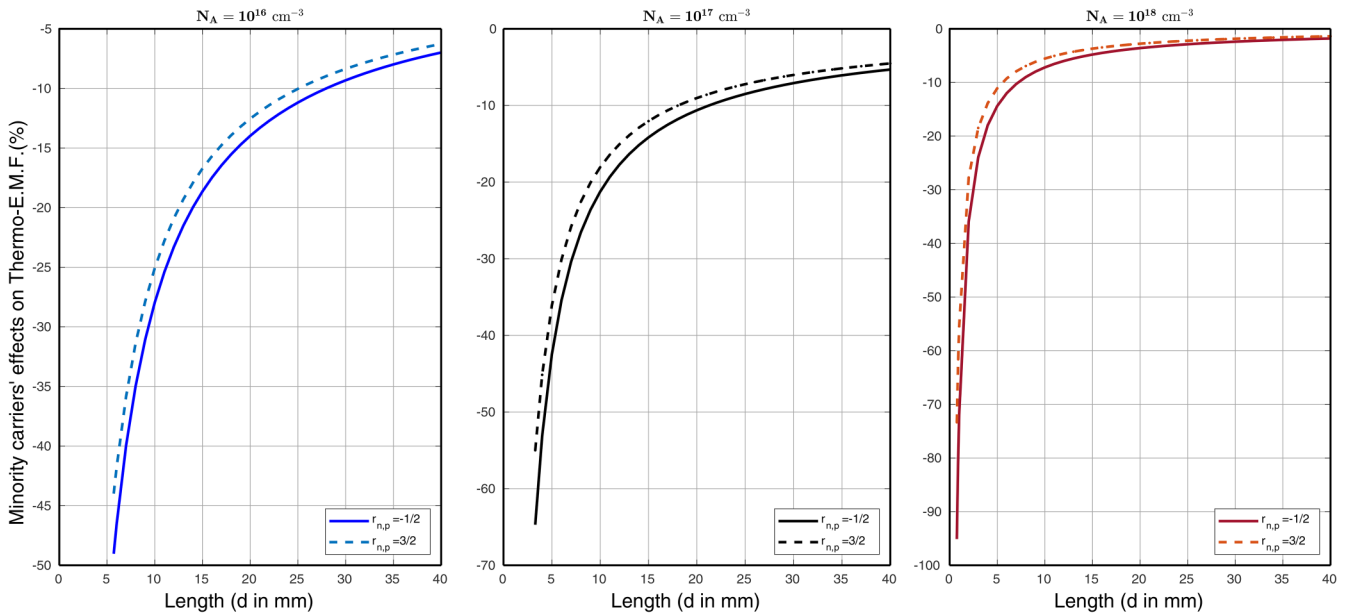

FIG. 1. The calculated counter-thermo-E.M.F. as a function of sample length when surface recombinations are weak ($L_0^{(p)} \ll d, L_S^{(p)}$) and for holes' concentrations $p_0 = 10^{16}$, $p_0 = 10^{17}$, and $p_0 = 10^{18}$ cm^{-3}.

recombination. In all three cases, its magnitude remains very important at high energy (solid line) and can reach up to 49%, 65%, and 95% of the classical thermo-E.M.F. of p-type silicon, respectively, for $N_A = 10^{16}$, $N_A = 10^{17}$, and $N_A = 10^{18}\,\mathrm{cm}^{-3}$ and when $d = 10 \times L_0^{(p)}$. This magnitude then decreases sharply as d increases until around $40 \times L_0^{(p)}$, where the decrease continues but much more slowly. Between the chosen sample length range, the magnitude of the counter-thermo-E.M.F. remains above 5% for $N_A = 10^{16}$ and $N_A = 10^{17}\,\mathrm{cm}^{-3}$ (respectively, 9.3% and 6.8% at $d = 80$ mm) but can decrease to around 2.3% when the sample length reaches 80 mm and when $N_A = 10^{18}\,\mathrm{cm}^{-3}$. In the case where the scattering mechanism by ionized impurities is predominant (dashed curve), the magnitude of the counter-thermo-E.M.F. is lower than when $r_{n,p} = -\frac{1}{2}$. The difference between the counter-thermo-E.M.F.s corresponding to $r_{n,p} = -\frac{1}{2}$ and $r_{n,p} = \frac{3}{2}$ was calculated over the sample length range and for each of the concentrations mentioned above. The results show that the difference decreases as the length of the silicon sample and the concentration of acceptors in its structure increase. For example, for a 12 mm length sample, this difference is 32.78, 18.08, and 4.19 μV/K, respectively, when the concentration of dopant elements is 10^{16}, 10^{17}, and $10^{18}\,\mathrm{cm}^{-3}$. However, the difference goes to 4.92, 2.71, and 0.63 μV/K in 80 mm long silicon and, respectively, for above doping impurity concentrations. From Ref. 33, the electrical resistivity of a p-semiconductor when $L_0^{(p)} \ll d, L_S^{(p)}$ is

$$\rho = \frac{1}{\sigma_p} + \frac{1}{\sigma_n}\frac{L_0^{(p)}}{d}. \tag{20}$$

It is then possible to express and calculate the dimensionless figure of merit of p-type silicon in the following form:

$$zT = \frac{\alpha^2}{\rho\kappa}T, \tag{21}$$

where ρ and κ are given by Eqs. (13) and (20), respectively. The Seebeck coefficient α is defined as follows:

$$\alpha = \alpha_p + \frac{\sigma_n}{\sigma_p}\alpha_n - \frac{\varepsilon_{g0}}{eT_0}\cdot\frac{L_0^{(p)}}{d} \tag{22}$$

The result of the calculation of zT of p-type silicon is shown in Fig. 2. Its values remain quite low of the order of 10^{-14}, 10^{-15}, and 10^{-16} when the concentration of the majority carriers is 10^{16}, 10^{17}, and 10^{18}, respectively. Nevertheless, this figure of merit increases with the length of the silicon sample and has larger values when the phonon scattering mechanism predominates. The dependence of zT on the predominant scattering mechanism also increases when using silicon of longer lengths.

If the characteristic length is proportional to the diffusion length; i.e., in other words, if there exists a real λ such that $L_S^{(p)} = \lambda L_0^{(p)}$, then from Eq. (18), the counter-thermo-E.M.F. becomes

$$\mathrm{E}_n = \left(\frac{\sigma_n}{\sigma_p}\alpha_n - \frac{\varepsilon_{g0}}{eT_0}\frac{\lambda L_0^{(p)}}{(\lambda+1)d}\right)\Delta T. \tag{23}$$

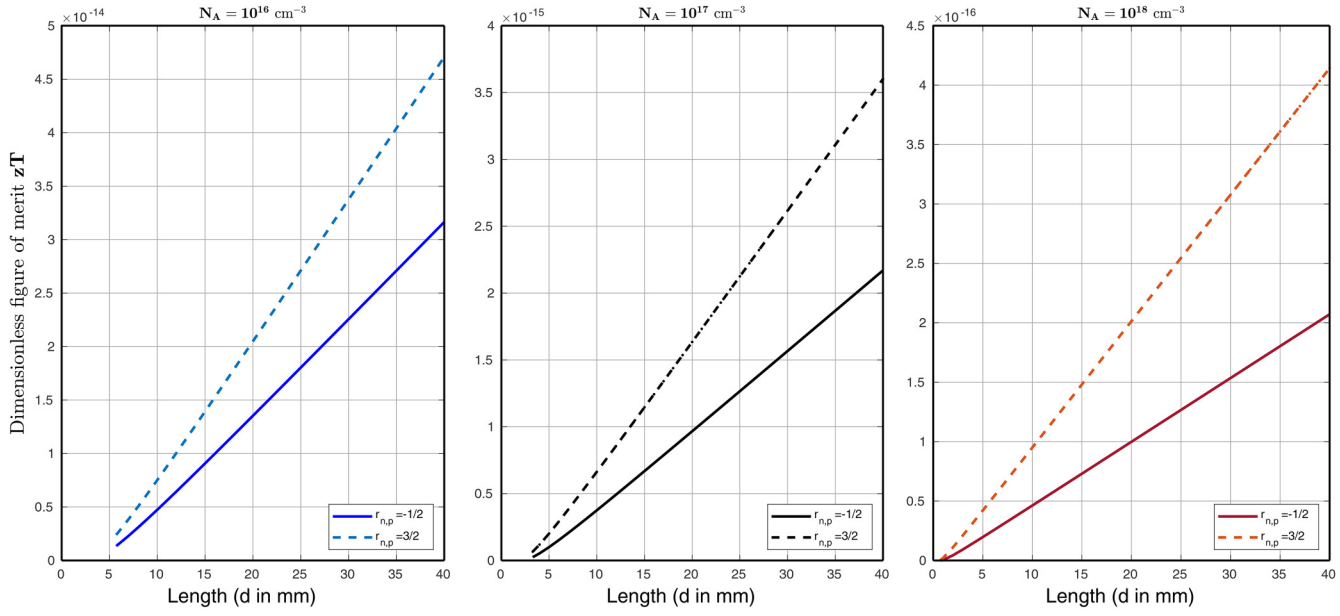

FIG. 2. Calculated zT as a function of sample length when surface recombinations are weak ($L_0^{(p)} \ll d, L_S^{(p)}$) and for holes' concentrations $p_0 = 10^{16}$, $p_0 = 10^{17}$, and $p_0 = 10^{18}\,\mathrm{cm}^{-3}$.

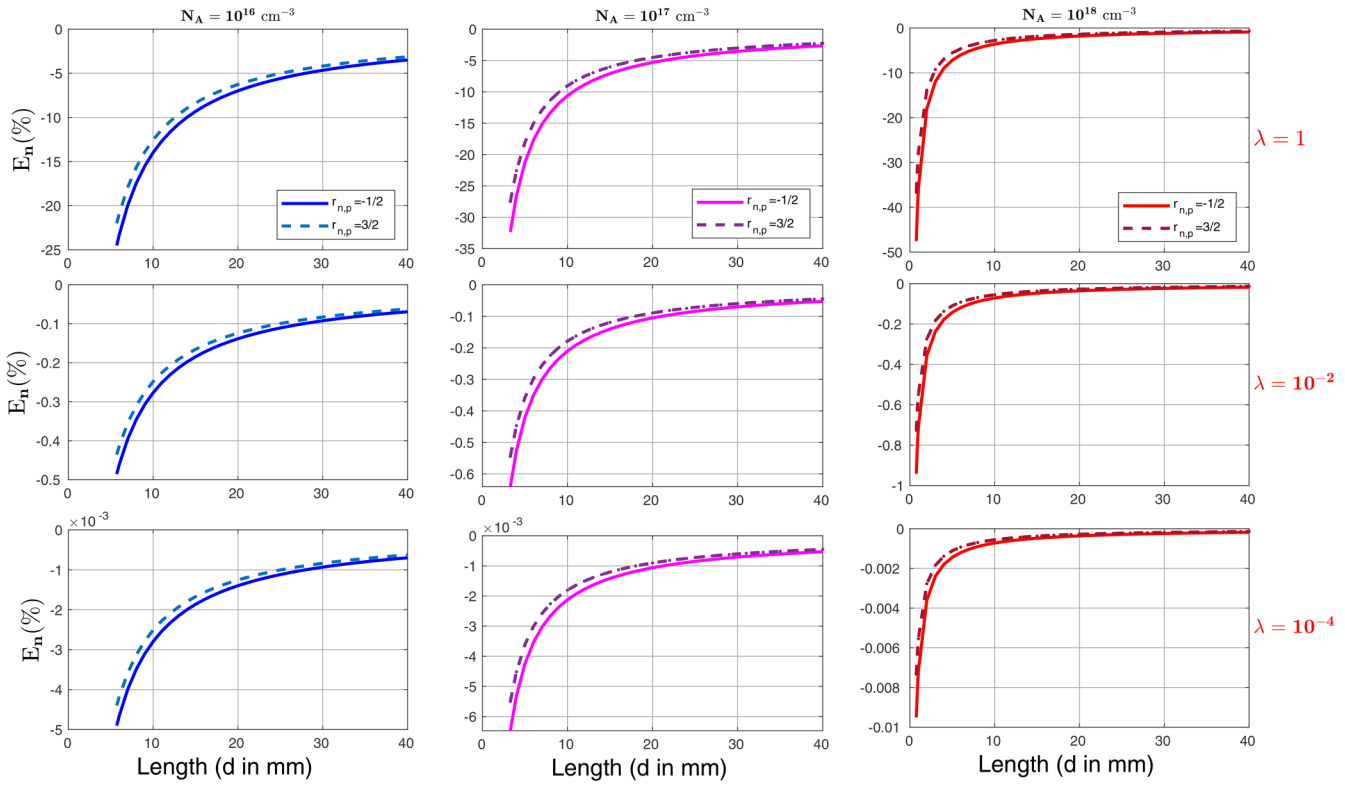

FIG. 3. Variation of the counter-thermo-E.M-F. as a function of sample length when $L_S^{(p)} = \lambda L_0^{(p)}$ and for $p_0 = 10^{16}$, $p_0 = 10^{17}$, and $p_0 = 10^{18}$ cm^{-3}.

The variations of $\frac{E_n}{\alpha_p \Delta T} \times 100$ with half the sample length corresponding to Eq. (20) are shown in the following Fig. 3 for four different values of λ (1, 10^{-2}, 10^{-4}). The first row corresponds to $\lambda = 1$, and the second and third correspond to $\lambda = 10^{-2}$ and $\lambda = 10^{-4}$, respectively. The columns correspond from left to right to dopings' density $N_A = 10^{16}$, $N_A = 10^{17}$, and $N_A = 10^{18}$ cm^{-3}. It is noted that when λ decreases, i.e., when recombinations intensify at the surface, the magnitude of the counter-thermo-E.M-F. decreases.

When $\lambda = 1$, the counter-thermo-E.M.F. remains significant for the three concentrations of the majority carriers and over the range of length d considered. If the concentration of dopants is $N_A = 10^{16}$ cm^{-3}, the magnitude of counter-thermo-E.M.F. decreases from 24.5% to 3.5% (from 22% to 3.13%) when d goes from $10 \times L_0^{(p)}$ to 40 mm and when $r_{n,p} = -\frac{1}{2}$ (when $r_{n,p} = \frac{3}{2}$). For the concentration of acceptors equal to 10^{17} cm^{-3}, that magnitude varies from 32.4% to 2.7% (27.5% to 2.3%) when half the length of the sample is changed from $10 \times L_0^{(p)}$ to 40 mm and when $r_{n,p} = -\frac{1}{2}$ (when $r_{n,p} = \frac{3}{2}$). Finally, if $N_A = 10^{18}$ cm^{-3} and d is changed from $10 \times L_0^{(p)}$ to 40 mm, the magnitude counter-thermo-E.M.F. also decreases but from 47.6% to 0.9% when the scattering mechanism by phonons predominates or from 36.7% to 0.7% if the scattering mechanism by ionized impurities predominates. When we assign to λ the values 10^{-2} and 10^{-4}, the magnitude of the counter-thermo-E.M.F. decreases significantly. It is of the order of 10^{-1}% for the first value of λ and of the order of 10^{-3}% for the second. Also it was noted that for silicon samples of length less than 60 mm, the order of magnitude of the counter-thermo-E.M.F as a percentage of the thermo-E.M.F. holes is 10 times the order of magnitude of λ. So, if $\lambda \ll 1$, that is, when the recombinations become very strong on the surface ($L_S^{(p)} \ll L_0^{(p)}, d$). The counter-thermo-E.M.F. tends toward $\frac{\sigma_n}{\sigma_p}\alpha_n \Delta T$, which is independent of the length of the semiconductor. Its magnitude in that case as a percentage of the classical thermo-E.M.F. of p-type silicon is of the order of 10^{-9}, 10^{-11}, and 10^{-13}% when the concentrations of the dopants are, respectively, 10^{16}, 10^{17}, and 10^{18} cm^{-3}. Then the counter-thermo-E.M.F. due to the presence of electrons in p-type silicon can be neglected and the classical theory of the thermo-E.M.F. of this type of semiconductor is valid only for small values of λ. When λ increases (recombinations decrease by the surface) and becomes very large ($\lambda \gg 1$), the counter-thermo-E.M.F. tends toward the following formula:

$$E_n = \left(\frac{\sigma_n}{\sigma_p}\alpha_n - \frac{\varepsilon_{g0}}{eT_0}\frac{L_S^{(p)}}{d}\right)\Delta T. \tag{24}$$

In summary, in a p-type semiconductor of very short length ($d \ll L_0^{(p)}$), only minority electrons contribute to the formation of

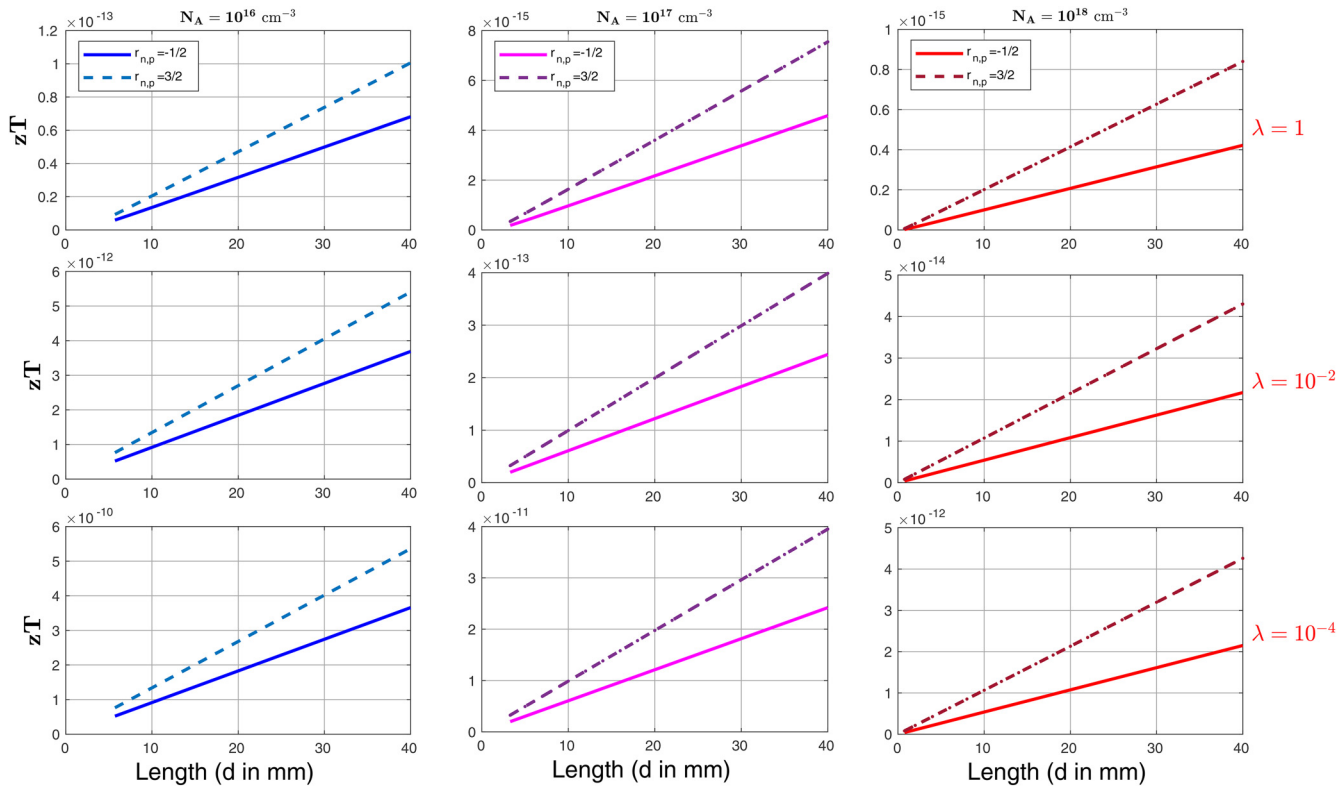

FIG. 4. Calculated zT as a function of sample length when $L_S^{(p)} = \lambda L_0^{(p)}$ and for holes' concentrations $p_0 = 10^{16}$, $p_0 = 10^{17}$, and $p_0 = 10^{18}$ cm^{-3}.

the thermo-E.M.F. But when the length of the semiconductor sample is large ($d \gg L_0^{(p)}$), these minority carriers are responsible for the formation of a counter-thermo-E.M.F. whose magnitude can be controlled through recombination processes. It is possible to considerably reduce this magnitude by treating the surfaces to favor surface recombinations.

Once more from Ref. 33, one can express the electrical resistivity of a p-type semiconductor when $d \gg L_0^{(p)}$ and $L_S^{(p)} = \lambda L_0^{(p)}$ as

$$\rho = \frac{1}{\sigma_p} + \frac{1}{\sigma_n}\frac{\lambda L_0^{(p)}}{(\lambda+1)d}. \tag{25}$$

Using Eqs. (13) and (25), one can express and calculate the dimensionless figure of merit zT of p-type silicon as in Eq. (21), but with α, define when $L_S^{(p)} = \lambda L_0^{(p)}$ by

$$\alpha = \alpha_p + \frac{\sigma_n}{\sigma_p}\alpha_n - \frac{\varepsilon_{g0}}{eT_0}\frac{\lambda L_0^{(p)}}{(\lambda+1)d}. \tag{26}$$

The figure of merit zT of p-type silicon for the four values of the parameter λ mentioned above is shown in Fig. 3. As for Fig. 4, from top to bottom, the rows correspond, respectively, at $\lambda = 1$, 10^{-2}, and 10^{-4}. The columns from left to right correspond to doping densities of 10^{16}, 10^{17}, and 10^{18} cm^{-3}. zT increases considerably when λ decreases, i.e., when the surface recombination rate increases. If $\lambda \ll 1$, then zT becomes independent of the sample length and can be expressed as

$$zT = \frac{\left(\alpha_p + \frac{\sigma_n}{\sigma_p}\alpha_n\right)^2 \sigma_p}{\kappa}. \tag{27}$$

The values of zT calculated from Eq. (27) are recorded in Table IV. These values remain lower than those obtained for the figure of merit of n-type silicon calculated in Ref. 11 for the same doping profile. They are significantly closer compared to those presented in Fig. 2.

TABLE IV. Values of the effective figure of merit calculated from Eq. (27).

N_A (cm^{-3})		10^{16}	10^{17}	10^{18}
zT	$r_{n,p} = -\frac{1}{2}$	9.80×10^{-5}	4.22×10^{-4}	9.52×10^{-3}
	$r_{n,p} = \frac{3}{2}$	1.44×10^{-4}	6.89×10^{-4}	1.90×10^{-3}

IV. CONCLUSION

The contribution due to the presence of minority charge carriers to the thermo-E.M.F. of a non-degenerate p semiconductor has been expressed in the steady state and when the quasi-neutrality condition is fulfilled. The expression found for that contribution depends on the electrical conductivity, the thermal conductivity, the thermopower, and the recombination rates of the minority carriers. However, it also depends on other parameters of the semiconductor such as its length, bandgap, the lattice thermal conductivity, and the thermal and electrical conductivities of the majority charge carriers. It is also observed that the counter-thermo-EMF always contributes to decreasing the magnitude of the classical thermo-E.M.F. $\alpha_p \Delta T$. In the case of p-type silicon, the counter-Thermo-E.M.F. cannot be neglected for the case of weak surface recombination. The dimensionless figure of merit zT in that specific case $(L_0^{(p)} \ll d, L_S^{(p)})$ is considerably altered due to the action of minority carriers. But, zT increases slightly with the length of the sample. The magnitude of the counter-Thermo-E.M.F. decreases when the length of the silicon and the concentration of the doping elements increase and when the recombination processes intensify in bulk or on the surface. For very high surface recombinations $(L_S^{(p)} \ll d, L_0^{(p)})$, the counter-thermo-E.M.F. becomes feeble but not null. In that case, its magnitude and zT are independent of the sample length. Furthermore, the values of zt are enhanced.

ACKNOWLEDGMENTS

The authors want to acknowledge the partial financial support of Consejo Nacional de Ciencia y Tecnología Mexico (CONACYT). The authors also thank Aarón Israel Díaz Cano for helpful discussions.

AUTHOR DECLARATIONS

Conflict of Interest

The authors have no conflicts to disclose.

Author Contributions

André Siewe Kamegni: Investigation (equal); Methodology (equal); Writing – original draft (equal). **Igor Lashkevych:** Investigation (equal); Methodology (equal); Validation (equal); Visualization (equal).

DATA AVAILABILITY

The data that support the findings of this study are available from the corresponding author upon reasonable request.

APPENDIX A: DETAILS ABOUT THERMO-E.M.F. EXPRESSION OF A p-TYPE SEMICONDUCTOR

For a bipolar semiconductor, the Thermo-E.M.F. is given by[38]

$$\mathrm{E} = \left(\frac{\sigma_n \alpha_n + \sigma_p \alpha_p}{\sigma_n + \sigma_p} - \frac{\varepsilon_{g0}}{eT_0} \frac{\sigma_p}{\sigma_n + \sigma_p} \frac{\frac{L_0}{d}(\gamma+1)\sinh\frac{d}{L_0}}{\frac{L_0}{d}\sinh\frac{d}{L_0} + \gamma\left[\cosh\frac{d}{L_0} + \frac{L_0}{L_S}\sinh\frac{d}{L_0}\right]} \right) \Delta T.$$

If the semiconductor is p-type, $\sigma_n \ll \sigma_p$ and $\frac{\sigma_n \alpha_n + \sigma_p \alpha_p}{\sigma_n + \sigma_p} \approx \alpha_p + \frac{\sigma_n}{\sigma_p}\alpha_n$. Also, $\frac{\sigma_p}{\sigma_n + \sigma_p} \approx 1$. Here, L_0 and L_S are diffusion length and characteristical length for bipolar semiconductors. Taking into account all these approximation, the expression of the Thermo-E.M.F. becomes

$$\mathrm{E} = \left(\alpha_p + \frac{\sigma_n}{\sigma_p}\alpha_n - \frac{\varepsilon_{g0}}{eT_0} \frac{\frac{L_0^{(p)}}{d}(\gamma^{(p)}+1)\sinh\frac{d}{L_0^{(p)}}}{\frac{L_0^{(p)}}{d}\sinh\frac{d}{L_0^{(p)}} + \gamma^{(p)}\left[\cosh\frac{d}{L_0^{(p)}} + \frac{L_0^{(p)}}{L_S^{(p)}}\sinh\frac{d}{L_0^{(p)}}\right]} \right) \Delta T.$$

By setting $\Gamma^{(p)} = \frac{\varepsilon_{g0}}{eT_0} \frac{\frac{L_0^{(p)}}{d}(\gamma^{(p)}+1)\sinh\frac{d}{L_0^{(p)}}}{\frac{L_0^{(p)}}{d}\sinh\frac{d}{L_0^{(p)}} + \gamma^{(p)}\left[\cosh\frac{d}{L_0^{(p)}} + \frac{L_0^{(p)}}{L_S^{(p)}}\sinh\frac{d}{L_0^{(p)}}\right]}$, Eq. (9) is found.

APPENDIX B: EXPRESSION OF THE PARAMETER $\gamma^{(p)}$

The parameter γ is defined for bipolar semiconductors as[33,38,47] $\gamma = \frac{e^2\kappa}{\xi\varepsilon_{g0}} \frac{\sigma_n + \sigma_p}{\sigma_n \sigma_p}$. For p-type semiconductors $(\sigma_n \ll \sigma_p)$ and considering the equivalence $\kappa \equiv \frac{\kappa}{k_B}$ established in Sec. III, the expression of that parameter turns into $\gamma^{(p)}$ given in Eq. (12).

APPENDIX C: CHARGE CARRIERS LIFETIME EXPRESSION

The charge carriers lifetime in a bipolar semiconductor is written as $\tau_0 = \left(\frac{1}{\tau_{bb}} + \frac{1}{\tau_{SRH}}\right)^{-1}$ where $\tau_{bb} = \frac{1}{k_d(n_0+p_0)}$ and $\tau_{SRH} = \left(\frac{k_n k_p N_t (n_0+p_0)}{k_n(n_0+n_1)+k_p(p_0+p_1)}\right)^{-1}$. In these equations, k_d, k_n, and k_p represent the capture coefficient of electrons by holes in direct transitions, the capture coefficient of electrons by recombination centers, and the capture coefficient of holes by recombination centers, respectively. Generally, $k_n \approx k_p$. When the energy level introduced by recombination centers coincides with the Fermi level, the concentrations of electrons and holes are, respectively, n_1 and p_1. For semiconductors with indirect bandgap like silicon, $\tau_{bb} \gg \tau_{SRH}$, i.e., $\frac{1}{\tau_{bb}} \ll \frac{1}{\tau_{SRH}}$, and the charge carriers' lifetime is reduced to $\tau_0 = \tau_{SRH}$. Moreover, if the semiconductor is p-type $p_0 \gg n_0$, $p_0 \gg n_1$, and $p_0 \gg p_1$, the carrier lifetime finally simplifies to $\tau_0 = \frac{1}{k_p N_t}$, which represents in a p-type semiconductor, the minority carriers lifetime.

REFERENCES

[1] S. Memon, *Advanced Thermoelectric Materials for Energy Harvesting Applications* (BoD–Books on Demand, 2019).
[2] Z. Soleimani, S. Zoras, B. Ceranic, S. Shahzad, and Y. Cui, "A review on recent developments of thermoelectric materials for room-temperature applications," Sustain. Energy Technol. Assess. **37**, 100604 (2020).
[3] S. Twaha, J. Zhu, Y. Yan, and B. Li, "A comprehensive review of thermoelectric technology: Materials, applications, modelling and performance improvement," Renew. Sust. Energy Rev. **65**, 698–726 (2016).
[4] C. R. Park, *Advanced Thermoelectric Materials* (John Wiley & Sons, 2019).
[5] E. Macia, *Thermoelectric Materials: Advances and Applications* (CRC Press, 2015).
[6] Z. Ren, Y. Lan, and Q. Zhang, *Advanced Thermoelectrics: Materials, Contacts, Devices, and Systems* (CRC Press, 2017).

[7]O. Brand, G. K. Fedder, C. Hierold, J. G. Korvink, and O. Tabata, *Thermoelectric Energy Conversion: Basic Concepts and Device Applications* (John Wiley & Sons, 2017).
[8]N. Hoang Pham, Ö. Vallin, J. Panda, M. V. Kamalakar, J. Guo, J. Luo, C. Wen, S.-L. Zhang, and Z.-B. Zhang, "High thermoelectric power factor of *p*-type amorphous silicon thin films dispersed with ultrafine silicon nanocrystals," J. Appl. Phys. **127**(24), 245304 (2020).
[9]F. Tohidi, S. G. Holagh, and A. Chitsaz, "Thermoelectric generators: A comprehensive review of characteristics and applications," Appl. Therm. Eng. **201**, 117793 (2022).
[10]C. B. Vining, "An inconvenient truth about thermoelectrics," Nat. Mater. **8**(2), 83–85 (2009).
[11]A. S. Kamegni and I. Lashkevych, "The thermo-E.M.F. of an n-type silicon: Assessment of the contribution due to the presence of minority carriers," Semicond. Sci. Technol. **38**(4), 045001 (2023).
[12]G. H. Julian, *Introduction to Thermoelectricity* (Springer, Berlin, 2016), Vol. 121.
[13]M. Henry, *Physique des semiconducteurs et des composants électroniques: Cours et exercices corrigés / Henry Mathieu,…Hervé Fanet,…* Sciences sup Sciences de l'ingénieur. Dunod, Paris, 2001.
[14]V. Zlatic and R. Monnier, *Modern Theory of Thermoelectricity* (OUP, Oxford, 2014).
[15]J.-P. Colinge and C. A. Colinge, *Physics of Semiconductor Devices* (Springer Science & Business Media, 2005).
[16]B. El Filali, O. Yu Titov, and Y. G. Gurevich, "Physics of charge transport in metal–monopolar (n-or p-type) semiconductor–metal structures," J. Phys. Chem. Solids **118**, 14–20 (2018).
[17]M. Lee, "Silicon: A revenant thermoelectric material?," J. Supercond. Novel Magn. **33**(1), 253–257 (2020).
[18]D. Narducci and F. Giulio, "Recent advances on thermoelectric silicon for low-temperature applications," Materials **15**(3), 1214 (2022).
[19]M. Saminathan, J. Palraj, P. Wesley, M. Moorthy, S. Perumal *et al.*, "Thermoelectric properties of p-type Si-rich higher manganese silicide for mid-temperature applications," Mater. Lett. **302**, 130444 (2021).
[20]C. Ngô and H. Ngô, *Physique des Semi-Conducteurs*, 4e ed. (Sciences de l'ingénieur. Dunod, 2012).
[21]B. G. Streetman and S. K. Banerjee, *Solid State Electronic Devices: Global Edition* (Pearson Education, 2016).
[22]R. Couderc, M. Amara, and M. Lemiti, "Reassessment of the intrinsic carrier density temperature dependence in crystalline silicon," J. Appl. Phys. **115**(9), 093705 (2014).
[23]C. D. Thurmond, "The standard thermodynamic functions for the formation of electrons and holes in Ge, Si, GaAs, and GaP," J. Electrochem. Soc. **122**(8), 1133 (1975).
[24]P. G. Burke, B. M. Curtin, J. E. Bowers, and A. C. Gossard, "Minority carrier barrier heterojunctions for improved thermoelectric efficiency," Nano Energy **12**, 735–741 (2015).
[25]J.-H. Bahk and A. Shakouri, "Minority carrier blocking to enhance the thermoelectric figure of merit in narrow-band-gap semiconductors," Phys. Rev. B **93**, 165209 (2016).
[26]V. F. Gantmakher and Y. B. Levinson, *Carrier Scattering in Metals and Semiconductors* (Elsevier, Amsterdam, 2012).
[27]M. Lundstrom, *Fundamentals of Carrier Transport*, 2nd ed. (Cambridge University Press, 2009).
[28]B. Qiu, Z. Tian, A. Vallabhaneni, B. Liao, J. M. Mendoza, O. D. Restrepo, X. Ruan, and G. Chen, "First-principles simulation of electron mean-free-path spectra and thermoelectric properties in silicon," Europhys. Lett. **109**(5), 57006 (2015).
[29]J. Zhou, B. Liao, and G. Chen, "First-principles calculations of thermal, electrical, and thermoelectric transport properties of semiconductors," Semicond. Sci. Technol. **31**(4), 043001 (2016).
[30]M. Grundmann, *Physics of Semiconductors* (Springer, Cham, 2015).
[31]P. Hofmann, *Solid State Physics: An Introduction* (Wiley-VCH Weinheim, Germany, 2015).
[32]S. Reggiani, M. Valdinoci, L. Colalongo, M. Rudan, and G. Baccarani, "An analytical, temperature-dependent model for majority-and minority-carrier mobility in silicon devices," VLSI Design **10**(4), 467–483 (2000).
[33]I. Lashkevych, O. Y. Titov, and Y. G. Gurevich, "Ohm's law for a bipolar semiconductor: The role of carrier concentration and energy nonequilibria," J. Electron. Mater. **46**, 585–595 (2016).
[34]M. Yao, M. Zebarjadi, and C. P. Opeil, "Experimental determination of phonon thermal conductivity and lorenz ratio of single crystal metals: Al, Cu, and Zn," J. Appl. Phys. **122**(13), 135111 (2017).
[35]C. J. Glassbrenner and G. A. Slack, "Thermal conductivity of silicon and germanium from 3°k to the melting point.," Phys. Rev. **134**, A1058–A1069 (1964).
[36]B. Liao, B. Qiu, J. Zhou, S. Huberman, K. Esfarjani, and G. Chen, "Significant reduction of lattice thermal conductivity by the electron-phonon interaction in silicon with high carrier concentrations: A first-principles study," Phys. Rev. Lett. **114**, 115901 (2015).
[37]H. M. van Driel, "Kinetics of high-density plasmas generated in si by 1.06- and 0.53-μm picosecond laser pulses," Phys. Rev. B **35**, 8166–8176 (1987).
[38]Y. G. Gurevich, I. Lashkevych, and A. Siewe Kamegni, "Non-linear in space temperature distribution and thermo-EMF in a bipolar semiconductor," Int. J. Thermophys. **43**(8), 1–17 (2022).
[39]Y. G. Gurevich, J. E. Velazquez-Perez, G. Espejo-López, I. N. Volovichev, and O. Y. Titov, "Transport of nonequilibrium carriers in bipolar semiconductors," J. Appl. Phys. **101**(2), 023705 (2007).
[40]J. P. McKelvey, *Solid State and Semiconductor Physics* (Krieger Pub Co, 1982).
[41]I. Lashkevych and Y. G. Gurevich, "Energy flux in semiconductors: Interaction of thermal and concentration nonequilibriums," Int. J. Heat Mass Transf. **92**, 430–434 (2016).
[42]Y. G. Gurevich and I. Lashkevych, "Sources of fluxes of energy, heat, and diffusion heat in a bipolar semiconductor: Influence of nonequilibrium charge carriers," Int. J. Thermophys. **34**(2), 341–349 (2013).
[43]P. T. Landsberg, *Recombination in Semiconductors* (Cambridge University Press, 1992).
[44]I. C. Ballardo Rodriguez, B. El Filali, O. Y. Titov, and Y. G. Gurevich, "Influence of thermal nonequilibrium on recombination, space charge, and transport phenomena in bipolar semiconductors," Int. J. Thermophys. **41**(5), 1–14 (2020).
[45]S. S. Li, *Semiconductor Physical Electronics* (Springer, New York, 2006).
[46]J. G. Fossum, "Computer-aided numerical analysis of silicon solar cells," Solid-State Electron. **19**(4), 269–277 (1976).
[47]I. Lashkevych and Y. G. Gurevich, "Linear electrical conductivity of a bipolar semiconductor: Heating and recombination," Int. J. Thermophys. **37**(1), 1–11 (2016).